Optics and Photonics Journal, 2014, 4, 195-212
Published Online August 2014 in SciRes. http://www.scirp.org/journal/opj
http://dx.doi.org/10.4236/opj.2014.48020

Scientific Research

Studies of Electron Energy Distribution Function (EEDF) in Lithium Vapor Excitation at 2S→3D Two-Photon Resonance

Mohamed A. Mahmoud[1], Kholoud A. Hamam[2]

[1]Physics Department, Faculty of Science, Sohag University, Sohag, Egypt
[2]Physics Department, Sciences Faculty for Girls, King AbdUlaziz University, Jeddah, KSA
Email: hameideg@yahoo.com

Received 29 May 2014; revised 27 June 2014; accepted 23 July 2014

Abstract

We have developed a computational model which quantitatively studies the Electron Energy Distribution Function (EEDF) in laser excited lithium vapor at 2s→3d two-photon resonance. A kinetic model has been constructed which includes essentially all the important collisional ionization, photoionization, electron collisions and radiative interactions that come into play when lithium vapor (density range 10^{13} - 10^{14} cm^{-3}) is subject to a sudden pulse of intense laser radiation (power range 10^{5} - 10^{6} $W{\cdot}cm^{-2}$) at wavelength 639.1 nm and pulse duration 20 ns. The applied computer simulation model is based on the numerical solution of the time-dependent Boltzman equation and a set of rate equations that describe the rate of change of the formed excited states populations. Using the measured values for the cross-sections and rate coefficients of each physical process considered in the model available in literature, relations are obtained as a function of the electron energy and included in the computational model. We have also studied the time evolution and the laser power dependences of the ion population (atomic and molecular ions) as well as the electron density which are produced during the interaction. The energy spectra of the electrons emerging from the interaction contains a number of peaks corresponding to the low-energy electrons produced by photoionization and collisional ionization such as assosicative and Penning ionization processes. The non-equilibrium shape of these electrons occurs due to relaxation of fast electrons produced by super-elastic collisions with residual excited lithium atoms. Moreover, a reasonable agreement between McGeoch results and our calculations for the temporal behaviour of the electron density is obtained.

Keywords

Two-Photon Resonance Excitation, Laser, Lithium, Collisional Ionization, Energy Pooling Photoionization, Electron Energy Distribution Function

How to cite this paper: Mahmoud, M.A. and Hamam, K.A. (2014) Studies of Electron Energy Distribution Function (EEDF) in Lithium Vapor Excitation at 2S→3D Two-Photon Resonance. *Optics and Photonics Journal*, **4**, 195-212.
http://dx.doi.org/10.4236/opj.2014.48020

1. Introduction

Generation of plasma in gases by intense laser pulses is a well-known optical phenomenon. The efficiency of this process can be increased by many orders of magnitude when the laser wavelength corresponds to an absorption line of ionized medium [1]. Laser-produced plasma sources are currently being developed to generate photons at a 13.5 nm wavelength to continue the development of faster computer chips. Utilizing the smallest wavelength for extreme ultraviolet lithography projection is the path to future progress in semiconductor technology [2].

On one hand, the electron energy distribution function is a topic of continuing interest to the plasma physics, fusion, and astrophysical communities because they can play an important role in the formation, evolution, and radiative properties of a wide variety of plasma sources. Non-Maxwellian electron energy distributions have been predicted or detected in diverse laboratory sources including tokomaks [3] [4], laser plasmas [5]-[7] and pulsed-power plasmas [8]-[10] as well as in astrophysical sources such as solar flares [11] [12] and active galactic nuclei [13], where they are generated by strong electric fields or resonant laser-plasma interactions. On the other hand, measurements of the EEDF are important for many applications, such as studies of absolute negative conductivity in photo plasma. This effect was predicted in the medium of a Li+Ar+N_2 mixture under optical resonant excitation of the 2s→2p transition in lithium [14] [15]. The additional interest in the EEDF for the photo plasma is related to the light-to-electric signal conversion [16] [17].

Two-photon excitation of Li(3d) state is a starting point for a variety of processes in lithium vapor. Under conditions of high atom densities (10^{15} cm^{-3}) and laser powers (10^6 $W{\cdot}cm^{-2}$), this excitation plays an important role in laser plasma production [18]-[20]. Recently, Labazan and Milosevic [21] studied the processes which occurred in lithium vapor under two-photon excitation of the Li(3d) state at 639.1 nm. In their experiment they used a pulsed dye laser pumped with excimer laser to excite the Li(3d) level by two-photon absorption at 639.1 nm. Density of lithium vapor was in the range (10^{13} - 10^{14} cm^{-3}) and laser powers (10^5 - 10^6 $W{\cdot}cm^{-2}$). The laser pulse duration was about 20 ns (FWHM), laser repetition rate was usually 5 Hz and the pulse energy was measured in the range 1 - 4 mJ at 639.1 nm. They had measured the radiation rates from lithium atomic states populated by two-photon excitation.

Theoretical modeling of alkali metal vapor ionization under resonant optical excitation was carried out in [22]-[25]. It was shown that there existed a competition of several ionization reactions: two-photon ionization of resonant states, associative resonant states, direct ionization by electron impact of the ground state, the resonant-state stepwise ionization by electron impact and photionization from high-lying excited states by resonance radiation.

More recently, Mahmoud *et al*. [26] presented a computational model to study the collisional ionization processes which occurred under 2s→2p excitation of lithium vapor excited with a nanosecond pulsed laser. Our interest in this work is primary to investigate the Electron Energy Distribution Function (EEDF) in lithium vapour excitation at 2s→3d two-photon resonance to determine conditions (namely lithium atom densities, laser energy, etc.) for the excitation processes because of its eventual importance in understanding ionization-guiding discharge experiments. This work studies two main subjects:

1) The influence of the ionization processes on the EEDF shape and the electron density in laser excited lithium by two-photon.

2) The dependence of EEDF and the ion density on the laser power and the lithium vapor density. In addition, we compare our results with that calculated by McGeoch [24]. The article is organized in the following way. In Section 2, we present theoretical model which includes the physical processes and the rate equations and the mathematical formula of the rate coefficients used to describe expected processes. In Section 3, we show our calculation results along with a discussion of various processes involved. Finally our conclusions are presented in Section 4.

2. The Theoretical Model of Laser Excited Lithium Vapour 2S→3D Transition

The energy level structure of lithium atom is well known [26]. Its low ionization potential provides little obstacles for multiphoton excitation and ionization. In the study of Labazan and Milosevic [21] Xe-Cl excimer laser pumped dye laser is used for the ionization of lithium vapor. Two photons at 639.1 nm will excite the lithium atom from the ground state 2S to the excited state 3D. Another 639.1 nm photon will ionize the lithium atom. The two-photon excitation rate $W^{(2)}$ in (s^{-1}) can be written as:

$$W^{(2)} = \sigma_{(2)} F^2 \tag{1}$$

where $\sigma_{(2)}$ and F represent the two-photon excitation cross section and the photon flux density respectively. The photon flux is given by,

$$F\left[\frac{\text{photon}}{\text{cm}^2 \cdot \text{sec}}\right] = \frac{I}{h\nu} = 3.3\times 10^{18} \cdot I\left[\text{W}\cdot\text{cm}^{-2}\right]$$

In this section, we consider the processes which occur in lithium vapour under two-photon excitation of the Li(3D) state at 639.1 nm. The molecular channel does not contribute to ionization processes according to the experimental conditions [20] [21].

2.1. Process Considered

1) The absorption of resonant photon.

$$\text{Li}(2\text{s}) + 2h\nu_{639.1} \rightarrow \text{Li}(3\text{d})$$

2) Photon ionization of the nl level.

$$\text{Li}(\text{nl}) + h\nu_{639.1} \rightarrow \text{Li}^+ + \text{e}$$

3) Associative ionization of 3d-3d collision.

$$\text{Li}(3\text{d}) + \text{Li}(3\text{d}) \rightarrow \text{Li}_2^+ + \text{e}$$

4) Collisional ionization (Penning ionization).

$$\text{Li}(3\text{d}) + \text{Li}(3\text{d}) \rightarrow \text{Li}^+ + \text{Li}(2\text{s}) + \text{e}$$

5) Reverse Energy pooling collisions.

$$\text{Li}(3\text{d}) + \text{Li}(2\text{s}) \rightarrow \text{Li}(2\text{p}) + \text{Li}(2\text{p})$$

6) Radiative decay of Li(3d).

$$\text{Li}(3\text{d}) \rightarrow \text{Li}(2\text{p}) + h\nu_{610.4\text{nm}}$$

7) Energy pooling collisions.

$$\text{Li}(2\text{p}) + \text{Li}(2\text{p}) \rightarrow \text{Li}(3\text{d}, 3\text{p}) + \text{Li}(2\text{s})$$

8) Super elastic collision (SEC):

The super elastic collision is described by the collision of a low energy electron with an excited atom. This process can be written as:

$$\text{Li}(\text{nl}) + \text{e}(\varepsilon_o) \rightarrow \text{Li}(2\text{s}) + \text{e}(\varepsilon) \quad \text{where } \varepsilon > \varepsilon_o.$$

9) Electron impact excitation:

This process is the inverse of superelastic collision process,

$$\text{Li}(\text{nl}) + \text{e}(\varepsilon) \rightarrow \text{Li}(\text{n}'\text{l}') + \text{e}(\varepsilon_o) \quad \text{where } \varepsilon > \varepsilon_o.$$

10) Electron impact ionization.

When an electron gains enough energy (through super-elastic collisions), which is equal to the ionization potential of the neutral atom, It can undergo an ionizing collision by electron impact process, resulting in a low energy electron of $(\varepsilon = \varepsilon_1 + \varepsilon_2 + \text{E}_{\text{ion}})$ and atomic ion.

$$\text{Li}(\text{nl}) + \text{e}(\varepsilon) \rightarrow \text{Li}^+ + \text{e}(\varepsilon_1) + \text{e}(\varepsilon_2)$$

where $\varepsilon = \varepsilon_1 + \varepsilon_2 + \text{E}_{\text{ion}}$ and E_{ion} is the ionization energy.

11) Radiative recombination.

$$\text{Li}^+ + \text{e}(\varepsilon) \rightarrow \text{Li}(\text{nl}) + h\upsilon$$

12) Three-body recombination.

$$\mathrm{Li}^{+}+\mathrm{e}(\varepsilon_1)+\mathrm{e}(\varepsilon_2)\rightarrow \mathrm{Li}(\mathrm{nl})+\mathrm{e}(\varepsilon)$$

where $3s \le nl \le 7d$.

For simplicity we have assumed that $\varepsilon_1 = \varepsilon_2$ in the electron impact ionization and its inverse three-body recombination processes. There are several assumptions which we use for mathematical description of excitation and ionization processes.

2.2. Rate Equations

The rate of change of population density of state 2s, 2p, 3d and the highly excited states nl is given by,

$$\begin{aligned}\frac{\mathrm{d}N(2s)}{\mathrm{d}t} &= N(3d)(W_{51}+A_{51})-N(2s)W_{15}+N(3p)A_{41}+N(2p)A_{21}\\ &\quad -N(2s)n_e(\varepsilon)k_{15}(\varepsilon)+N(3d)n_e(\varepsilon)k_{51}(\varepsilon)+\frac{1}{2}N^2(3d)k_{PI}\\ &\quad +\frac{1}{2}N^2(2p)k_{EP}-N(2s)N(3d)k_{REP}-N(2s)n_e(\varepsilon)k_{1c}(\varepsilon)\end{aligned} \tag{2}$$

$$\begin{aligned}\frac{\mathrm{d}N(2p)}{\mathrm{d}t} &= N(3d)A_{52}-N(2p)n_e(\varepsilon)k_{21}(\varepsilon)+N(2s)n_e(\varepsilon)k_{12}(\varepsilon)\\ &\quad +\frac{1}{2}N^2(3d)k_{PI}-\frac{1}{2}N^2(2p)k_{EP}+N(2s)N(3d)k_{REP}\\ &\quad -N(2p)\sigma_{2c}^{(1)}F-N(2s)n_e(\varepsilon)k_{2c}(\varepsilon)\end{aligned} \tag{3}$$

$$\begin{aligned}\frac{\mathrm{d}N(3d)}{\mathrm{d}t} &= N(2s)W_{15}-N(3d)(W_{51}+A_{51})-N(3d)A_{52}+N(2s)n_e(\varepsilon)k_{15}(\varepsilon)\\ &\quad -N(3d)n_e(\varepsilon)k_{51}(\varepsilon)-\frac{1}{2}N(3d)^2k_{AI}-\frac{1}{2}N(3d)^2k_{PI}-N(3d)\sigma_{5c}^{(1)}F\\ &\quad -\frac{1}{2}N^2(2p)k_{EP}-N(2s)N(3d)k_{REP}-N(3d)n_e(\varepsilon)k_{5c}(\varepsilon)\end{aligned} \tag{4}$$

$$\begin{aligned}\frac{\mathrm{d}N(n)}{\mathrm{d}t} &= \sum_{n>m}N(n)n_e(\varepsilon)k_{nm}(\varepsilon)-\sum_{m>n}N(m)n_e(\varepsilon)k_{mn}(\varepsilon)-\sum_{n>m}A_{nm}N(n)-\sum_{n}N(n)n_e(\varepsilon)k_{nc}(\varepsilon)\\ &\quad -\sum_{n>2}N(n)\sigma_{nc}^{(1)1cp}F+N_{\mathrm{Li}^+}n_e(\varepsilon)\sum_{n}\left[n_e(\varepsilon)k_{cn}(\varepsilon)+k_{RD}(\varepsilon)\right]\end{aligned} \tag{5}$$

The rate of growth of the molecular ion and the atomic ion is given by,

$$\frac{\mathrm{d}N(\mathrm{Li}_2^+)}{\mathrm{d}t}=\frac{1}{2}\left(N(3d)\right)^2k_{AI} \tag{6}$$

$$\frac{\mathrm{d}N(\mathrm{Li}^+)}{\mathrm{d}t}=\frac{1}{2}N^2(3d)k_{PI}+\sum_{n>2}N(n)\sigma_{nc}^{(1)}F+\sum_{n}N(n)n_e(\varepsilon)k_{nc}(\varepsilon) \tag{7}$$

where,

$N(2s), N(2p), N(3d)$ and $N(n)$ are the population density of levels 2s, 2p, 3d and nl, respectively.

$n_e(\varepsilon)$ represents the electron density as a function of electron energy (ε).

W_{15} is the stimulated absorption rate coefficient from 2s to 3d level (sec^{-1}).

W_{51} is the stimulated emission rate coefficient from 3d to 2s level (sec^{-1}).

A_{21} Einstein coefficient for spontaneous emission for the transition 2p to 2s (sec^{-1}).

A_{51} Einstein coefficient for spontaneous emission for the transition (3d to 2s) (sec^{-1}).

A_{41} Einstein coefficient for spontaneous emission for the transition 3p to 2s (sec^{-1}).

A_{52} Einstein coefficient for spontaneous emission for the transition 3d to 2p (sec^{-1}).

A_{nm} Einstein coefficient for spontaneous emission for the transition n→m (sec^{-1}).
k_{EP} represents the energy pooling collisions rate coefficient ($cm^3 \cdot sec^{-1}$).
k_{REP} represents the reverse energy pooling collisions rate coefficient ($cm^3 \cdot sec^{-1}$).
k_{AI} represents the association ionization rate coefficient ($cm^3 \cdot sec^{-1}$).
k_{PI} represents Penning ionization rate coefficient for level n ($cm^3 \cdot sec^{-1}$).
k_{51} represents the electron collision rate coefficient for transition from (3d→2s) as a function of electron energy (ε) ($cm^3 \cdot sec^{-1}$).
k_{15} represents the electron collision rate coefficient for transition from (2s→3d) as a function of electron energy (ε) ($cm^3 \cdot sec^{-1}$).
k_{5c} represents electron collision ionization rate coefficient for level 3d ($cm^3 \cdot sec^{-1}$).
k_{1c} represents electron collision ionization rate coefficient for level 2s ($cm^3 \cdot sec^{-1}$).
$k_{nc}(\varepsilon)$ represents electron collision ionization rate coefficient for level n ($cm^3 \cdot sec^{-1}$).
k_{nm} represents the electron collision rate coefficient for transition from (n→m) as a function of electron energy (ε) ($cm^3 \cdot sec^{-1}$).
$k_{mn}(\varepsilon)$ represents the electron collision rate coefficient for transition from (m→n) as a function of electron energy (ε) ($cm^3 \cdot sec^{-1}$).
$\sigma_{nc}^{(1)}$ represents the photon ionization cross-section for level n (cm^2).
$\sigma_{2c}^{(1)}$ represents the single photon ionization cross-section for level 2p (cm^2).
k_{cn} represents the three body recombination rate coefficient for level n ($cm^6 \cdot sec^{-1}$).
k_{RD} represents the radiative recombination rate coefficient ($cm^3 \cdot sec^{-1}$).
N_{Li^+} represents the density of atomic ions.
$N_{Li_2^+}$ represents the density of molecular ions.
F is the photon flux (photon/($cm^2 \cdot sec$)).

The electron energy distribution function equation (EEDF) is given by:

$$\begin{aligned}\frac{\mathrm{d}n_e(\varepsilon)}{\mathrm{d}t} &= \sum_{m>n} N(m)n_e(\varepsilon)k_{nm}(\varepsilon) - \sum_{m<n} N(n)n_e(\varepsilon)k_{mn}(\varepsilon) \\ &+ \sum_n N(n)n_e(\varepsilon)k_{nc}(\varepsilon) + \frac{1}{2}N^2(3d)k_{PI} + \frac{1}{2}N^2(3d)k_{AI} \\ &+ \sum_{n>2} N(n)\sigma_{nc}^{(1)}F - N_{Li^+}n_e(\varepsilon)\sum_n\left[n_e(\varepsilon)k_{cn}(\varepsilon) + k_{RD}(\varepsilon)\right]\end{aligned} \tag{8}$$

The normalization conditions are given by:

$$N_0 = \sum_n N(n) + N(Li^+) \tag{9}$$

$$\int_0^\infty n_e(\varepsilon)\varepsilon^{1/2}\mathrm{d}\varepsilon = 1 \tag{10}$$

where N_0 is the density of Li atomic vapour. Note that the factor 1/2 with k_{EP} and k_{AI} corrects for possible double counting of each colliding pair of identical particles [27].

2.3. Effects of EEDF on Collisional Rates

To calculate the electron energy distribution function, numerous data have to be compiled from the literature to be fed into the Boltzmann equation computational code [28]. By the use of suitable approximations for the energy dependence of the cross sections, the rate coefficients can be expressed by simple analytical formula. The rates of collisional process in plasma are given by the product of the plasma electron density n_e and the rate coefficient $\langle v\acute{o}\rangle$ of the particular process. The rate coefficient is determined by integrating an energy-dependent collision cross section $\acute{o}(\varepsilon)$ over the electron energy distribution function [29].

$$\langle v\acute{o}\rangle = \int_{\Delta E}^\infty v\sigma(\varepsilon)f(\varepsilon)\mathrm{d}\varepsilon\left[\mathrm{cm}^3\cdot\mathrm{s}^{-1}\right] \tag{11}$$

where v and ε are the velocity and energy, of the incident electron respectively. The lower limit of the integration is the threshold energy of the process for collisional excitation and ionization.

For single-temperature plasmas with Maxwellian electron energy distributions, de-excitation and recombination rates can be obtained directly from collisional excitation and ionization rate coefficients through detailed balance. For plasmas that have electrons in non-Maxwellian distributions, the cross sections of these reverse rates must be integrated over the entire electron energy distribution. By the use of suitable approximation for the energy dependence of the cross sections, the corresponding rate coefficients can be expressed by simple analytical formula.

The cross sections for excitation by electron impact $\delta_{\mathrm{nm}}^{\mathrm{ex}}$ are linearly approximated in the energy range of interest [29]:

$$\delta_{\mathrm{nm}}^{\mathrm{ex}}(\varepsilon) = \mathrm{C}_{\mathrm{nm}}(\varepsilon - \varepsilon_{\mathrm{s}}) \qquad \varepsilon > \varepsilon_{\mathrm{s}} = E_n - E_m \tag{12}$$

Here, C_{nm} is the excitation cross section constant and ε_s the energy threshold. The excitation rate coefficient is obtained by integration with respect to Maxwellian energy distribution:

$$k_{nm} = 4\left(\frac{k_B T_e}{2\pi m_e}\right)^{1/2} C_{nm}(\varepsilon_s + 2k_B T_e)\exp\left[-\varepsilon_s / k_B T_e\right] \tag{13}$$

The rate coefficient k_{mn} for the reverse reaction, superelastic collisions is obtained by the principle of detailed balance as follows:

$$k_{nm} = k_{mn}\frac{g_m}{g_n}\exp\left[(E_n - E_m)/k_B T\right] \tag{14}$$

where g_n and g_m are the statistical weights of the upper and lower levels, respectively.

For the ionization of excited states by electron impact we use the empirical formula given by Vriens and Smeets [30] for the cross section and rate coefficients:

$$\sigma_{nc} = \frac{6.5\times10^{-14}}{\varepsilon + 3.25E_i}\left(\frac{5}{E_i} - \frac{1}{\varepsilon} - \frac{2E_i}{3\varepsilon^2}\right) \tag{15}$$

where $E_i = 5.18 - E_n$ $\varepsilon \geq E_i$.

The reverse reaction, recombination by a three-particle collision, is obtained by the detailed balancing of ionization:

$$\frac{k_{nc}}{k_{cn}} = \left(\frac{2\pi m_e}{h^2}\right)^{3/2}\frac{2g_+}{g_n}\exp\left[\frac{-E_{+n}}{k_B T_e}\right] \tag{16}$$

where g_n and g_+ are the statistical weights of the neutral atomic and the atomic ion respectively.

For the radiative recombination rate coefficients we have used the empirical formula given by Drawin [31]:

$$k_{rd} = 2.07\times10^{-11} Z^2 T_e^{-\frac{1}{2}}\varphi(u_x) \tag{17}$$

$$\varphi(u_x) = -\sum_{n=1}\frac{u_x}{n^3}\mathrm{e}^{\left(\frac{u_x}{n^2}\right)}E_n\left(-\frac{u_x}{n^2}\right) \tag{18}$$

and $u_x = 1.58 \times 10^5$ $E_i^H = 13.59$ eV , Z is the atomic number of the neutral atom and T is the gas temperature in K˚.

On the other hand the values of the rate coefficients of collisional ionization, energy pooling collisions and processes in our model are indicated in **Table 1**.

3. Results and Discussion

The set of equations which was mentioned previously is solved numerically under the experimental conditions of Labazan and Milosevic [21]. In this instance the initial lithium vapor density was assumed to be 3×10^{13} - 7×10^{14} cm^{-3}, the laser power changes from 1×10^5 to 1×10^6 $\mathrm{W\cdot cm}^{-2}$, the temperature varied from 760 K˚ - 880 K˚ and the energy of single pulse (E) varied from 1→4 m Joule. The laser intensity (I) is given by $\mathrm{I} = \frac{E}{\tau\times\pi r^2}$,

Table 1. Kinetic processes in lithium ionization model.

Process	Cross Section	Reference
Two photon absorption $\sigma_{(2)}$: $Li(2s)+2h\nu \rightarrow Li(3d)$	6.25×10^{-31} cm$^4\cdot$s	[32]
Spontaneous emission for the transition 2p→2s: A_{21}	0.186×10^{7} sec^{-1}	[33]
Spontaneous emission for the transition 3d→2p: A_{52}	2.389×10^{7} sec^{-1}	[33]
Spontaneous emission for the transition 3p→2s: A_{42}	0.39×10^{6} sec^{-1}	[33]
Spontaneous emission for the transition 3d → 2s: A_{51}	2.53×10^{2} sec^{-1}	[34]
Associative ionization $k_{AI}: Li(3d)+Li(3d)\rightarrow Li_2^+ + e^-$	7×10^{-14} cm^2	[35]
Penning ionization $k_{PI}: Li(3d)+Li(3d)\rightarrow Li^+ + Li(2s)+e^-$	14×10^{-14} cm^2	[35]
Energy pooling $k_{EP}: Li(2p)+Li(2p)\rightarrow Li(3p,3d)+Li(2s)$	7.8×10^{-15} cm^2	[36]
Reverse Energy pooling $K_{REP}: Li(3p,3d)+Li(2s)\rightarrow Li(2p)+Li(2p)$	6×10^{-16} cm^2	[37]
Single photon ionization 3s	1.48×10^{-18} cm^2	[38]
Single photon ionization 4s	1.40×10^{-18} cm^2	[38]
Single photon ionization 5s	1.33×10^{-18} cm^2	[38]
Single photon ionization 2p	12.50×10^{-18} cm^2	[38]
Single photon ionization 3p	28.10×10^{-18} cm^2	[38]
Single photon ionization 4p	41.7×10^{-18} cm^2	[38]
Single photon ionization 5p	56.2×10^{-18} cm^2	[38]
Single photon ionization 3d	18.2×10^{-18} cm^2	[38]
Single photon ionization 4d	36.2×10^{-18} cm^2	[38]

where τ is the laser pulse duration and r is the laser beam radius. Under these conditions, the laser light was tuned to the two-photon resonance 2s→3d, at λ = 639.1 nm. The rate equation for the electron energy distribution function (8) is divided into 54 equations, where the ionization energy of Li = 5.39 eV and the energy step equal 0.1 eV. We calculate 1) the electron energy distribution function and its dependence on the laser intensity and lithium vapor density., 2) the effect of laser power and the time on the atomic ion (Li^+) and the molecular ion $\left(Li_2^+\right)$, 3) the effect of laser power and the lithium vapor density on the time evolution of the electron density which generated during the laser interaction with lithium vapor.

3.1. The Dependence of the Electron Energy Distribution Function on the Lithium Atomic Vapor and Laser Power

The electron energy distribution function as a function of lithium atomic vapor after 20 ns and laser power 1×10^5 W·cm^{-2} is plotted and shown in **Figure 1**. From this figure we note that the spectral structure is observed with certain peaks (A, B, C, D, and E) lying at energies 0.35, 1.1, 1.75, 2.5 and 3 eV respectively. The energy distribution of the electrons produced in peak A is centering at a mean energy E ≈ 0.35 eV by photon ionization processes which is described by the following equation.

$$Li(3d,3p,3s)+h\upsilon_{639.1}\rightarrow Li^+ + e$$

Also the peak B corresponds to electrons produced by photon ionization processes of (5s, 4d, 4p, 4s).

$$Li(5s,4d,,4p,4s)+h\upsilon_{639.1}\rightarrow Li^+ + e$$

While the peak C corresponds to single photon ionization.

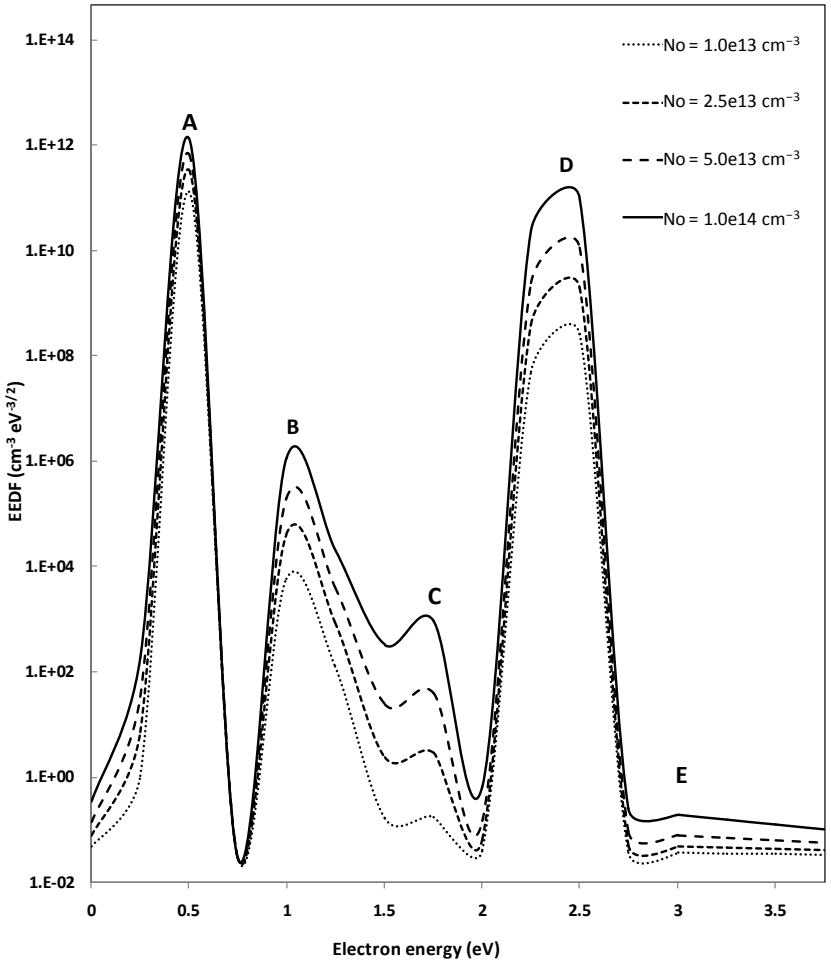

Figure 1. The dependence of the Electron Energy Distribution Function on the lithium vapor density after 20 n sec from the laser pulse and laser power 1×10^5 W·cm^{-2}.

$$\mathrm{Li}(5\mathrm{p}) + \mathrm{h}\nu_{639.1} \rightarrow \mathrm{Li}^+ + \mathrm{e}$$

The peak D corresponds to the electrons produced by Penning and associative ionization of Li(3d**)** which described by the following collision.

$$\mathrm{Li}(3\mathrm{d}) + \mathrm{Li}(3\mathrm{d}) \rightarrow \mathrm{Li}^+ + \mathrm{Li}(2\mathrm{s}) + \mathrm{e}$$

$$\mathrm{Li}(3\mathrm{d}) + \mathrm{Li}(3\mathrm{d}) \rightarrow \mathrm{Li}_2^+ + \mathrm{e}$$

While the peak E is attributed to the superelastic collisions.

$$\mathrm{Li}(\mathrm{nl}) + \mathrm{e}(\varepsilon_o) \rightarrow \mathrm{Li}(2\mathrm{s}) + \mathrm{e}(\varepsilon) \quad \text{where } \varepsilon > \varepsilon_o.$$

We assume that the interaction started with the absorption of laser photons by Li(2s) excited to Li(3d) through two-photon resonance process. We assume that the most important source of population of the Li(3d) state is the laser excitation, atoms can make many interactions like Penning, associative ionization, photoionization, decay to Li(2p) (life time $\tau_{3d\text{-}2p}$ = 16.7 ns [20], may collide with Li(2s) in reverse energy pooling reaction to form Li(2p) atoms which is the main source of highly excited atoms through energy pooling interactions, also Li(3d) atoms may collide with Li(2s) to create Li(3p) through energy transfer collisions [21], finally super elastic collisions and photoionization processes of all excited states can take place during the interaction.

The dependence of the electron energy distribution function on the laser power after 20 ns and lithium vapor density 3×10^{13} cm^{-3} is indicated in **Figure 2**. From this figure we show that, as the laser power increases, the

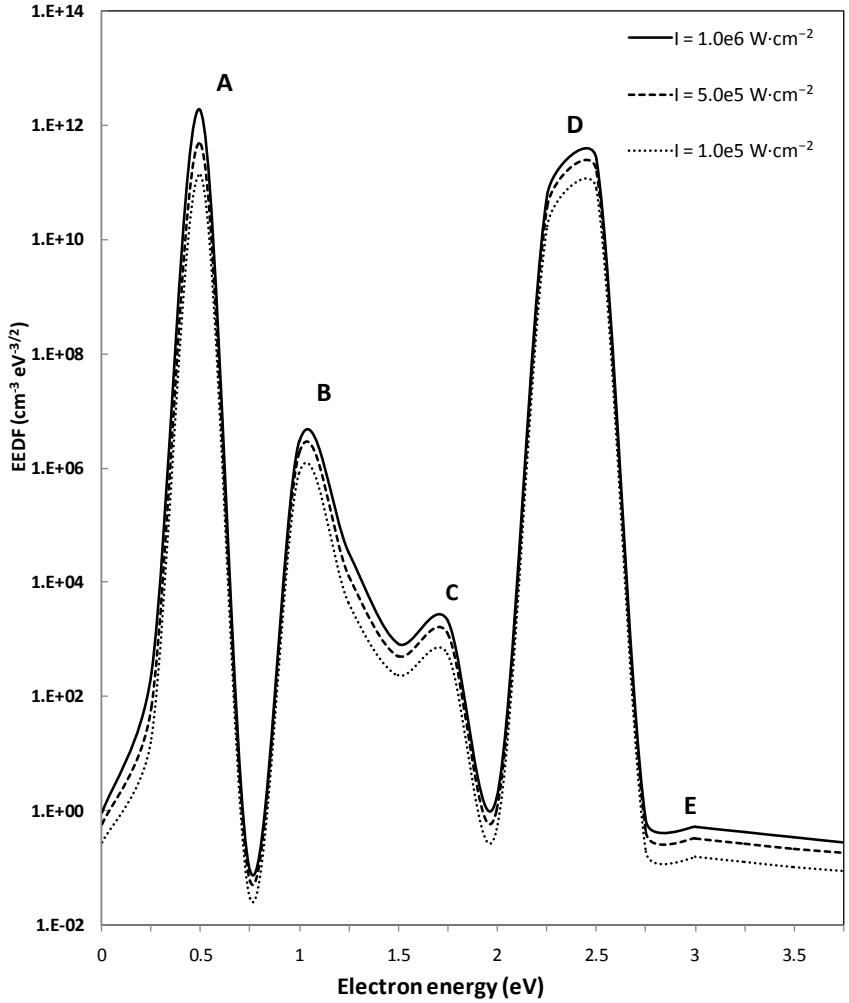

Figure 2. Electron Energy Distribution Function after 20 n sec from the laser pulse at different values of laser power and lithium vapor density 3×10^{13} cm^{-3}.

value of the electron energy distribution increases at EEDF corresponding to peaks, B, C and E. This result indicates the dependence of the occurrence of some physical processes on the laser power which turn results in the appearance of such peaks in EEDF. These peaks are attributed to some physical processes which contribute to the population and depopulation of the various excited states considered in this analysis. The figures illustrates the role of the photoioniation process in EEDF formation in the case when J_{ph} is for an order of magnitude greater than the ionization flux due to electron impact $J_{ei} = k_{c,2p}N(2p)n_e$. Photoionization from the Li (3P) and Li(3d) states produces electrons with energy ~0.3 eV. As one can see, a peak is formed on EEDF around this energy. However the interesting point from our point of view is that, the photoionization and collisional ionization are the dominant processes during the plasma formation in laser excited lithium atoms [15] [16].

3.2. The Dependence of the Atomic Ions (Li^+) Density on the Atomic Lithium Vapor and Laser Power

The growth rate of the atomic ions (Li^+) density as a function of lithium vapor density is shown in **Figure 3** for different values of irradiation time. From this figure it can be seen that the atomic ions (Li^+) density show that as the lithium density increases the ion density Li^+ increases and the curves show almost the same behavior with descending values of lithium vapor density for different values of time. Also it is observed that the density of atomic ions (Li^+) increases with the laser power as indicates in **Figure 4** for different values of time. This behavior is due to the Li^+ mainly produced by the photoionization and laser induced Penning ionization processes

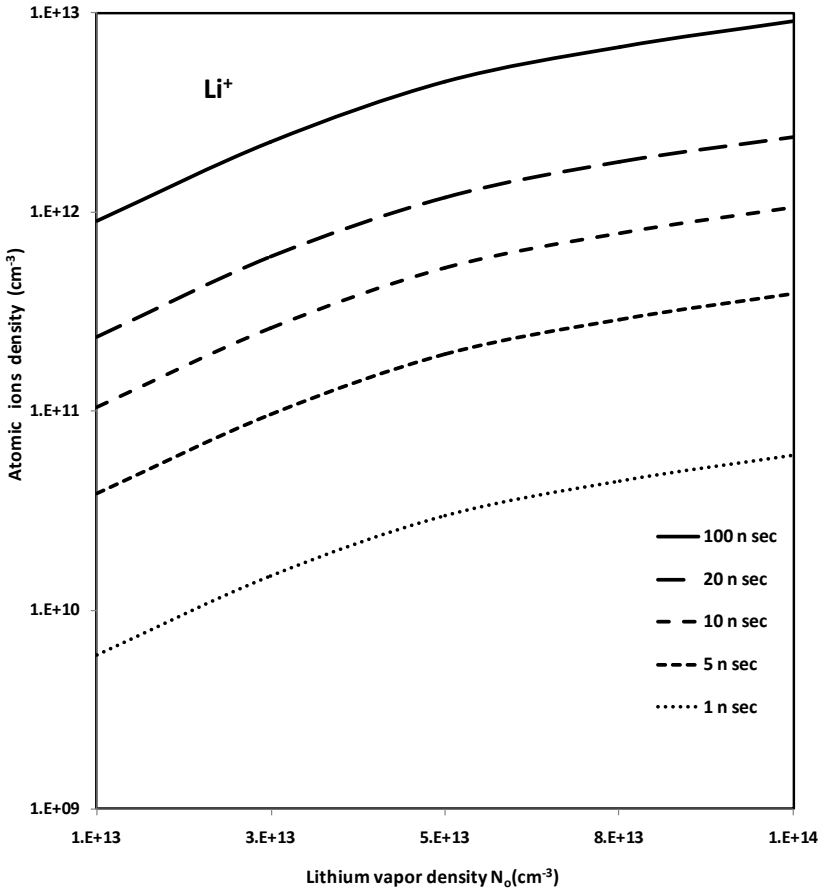

Figure 3. Variation of Atomic ions density Li^+ with Lithium vapor density N_o at different time intervals and laser power 1×10^5 W·cm^{-2}.

[17]. Collisions of highly-excited atoms with resonantly excited ones may result in Penning ionization where nl states are populated in energy pooling collisions of two Li(2p) atoms [21].

3.3. The Time Evolution of the Atomic Ion Li^+

The growth rate of the Li^+ as a function of time is indicated in **Figure 5** for different values of laser power. From this figure it can be seen that the (Li^+) shows a fast increase during the early stages of the interaction up to 5 ns followed by a linear increase up to 10 ns. Immediately after this time the density of Li^+ density shows a slow increase during the late stage of the irradiation time. This behavior is due to the Li^+ mainly produced by the Penning ionization and photionization processes as follows:

$$\mathrm{Li}(3\mathrm{d}) + \mathrm{Li}(3\mathrm{d}) \rightarrow \mathrm{Li}^+ + \mathrm{Li}(2\mathrm{s}) + \mathrm{e} \quad (\mathrm{PI})$$

$$\mathrm{Li}(\mathrm{nl}) + \mathrm{h}\nu \rightarrow \mathrm{Li}^+ + \mathrm{e} \quad (\mathrm{PHO})$$

where nl states are populated in energy pooling collisions of two Li(3d) atoms:

$$\mathrm{Li}(2\mathrm{p}) + \mathrm{Li}(2\mathrm{p}) \rightarrow \mathrm{Li}(\mathrm{nl}) + \mathrm{Li}(2\mathrm{s}) \quad (\mathrm{EP})$$

In general the figure shows the same behavior for almost values of the irradiation time.

3.4. The Molecular ions $\left(Li_2^+\right)$ Density as a Function of Lithium Vapor Density

Density of the molecular ions $\left(Li_2^+\right)$ variation with lithium vapor density is illustrated in **Figure 6** at laser power 1×10^5 W·cm^{-2}. From this figure we can see that the Li_2^+ density increases rapidly with increasing of

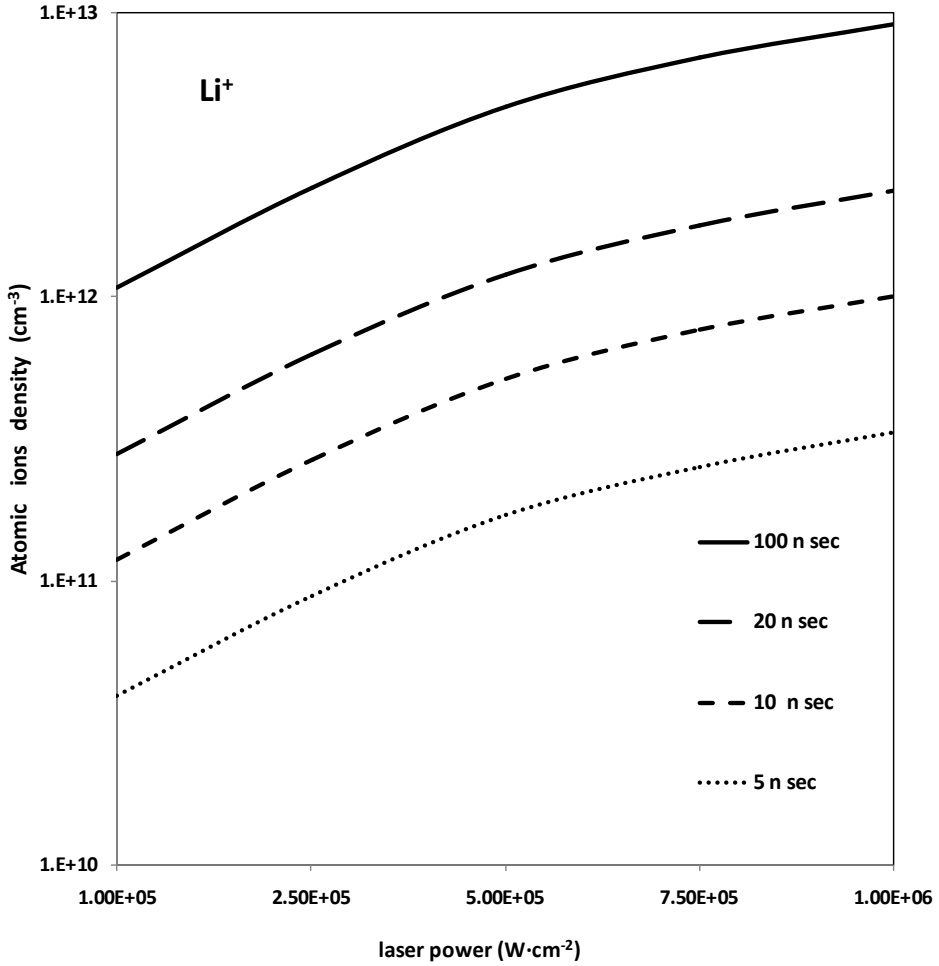

Figure 4. Variation of Atomic ions density Li^+ with laser power at different time intervals and lithium vapour density 7×10^{14} cm^{-3}.

lithium vapor density, while the density of molecular ions is approximately constant with the variation of laser power where the molecular ions are produced from associative ionization (AI). On the hand, in lithium unlike the rest of the alkali metals, the reaction of the association ionization of two resonant excited atoms is not important at T (gas temperature) < 0.1 eV, due to a considerable energy deficit (~0.7 eV) which diminishes its efficiency [16].

3.5. The Time Evolution of the Molecular Ion Li_2^+

The growth rate of the molecular ion Li_2^+ as a function of time is illustrated in **Figure 7** for different values of laser power. From this figure, we can see that the Li_2^+ density shows a fast increase during the period 0.1 ns up to 5 ns followed by a linear increase up to 20 ns. Immediately after this time the Li^+_2 density shows a slow increase during the late stages of the irradiation time. An understanding of this behavior can be attained by considering that the main processes for producing these molecular ions are associative ionization (AI) process as follows:

$$\mathrm{Li}(3\mathrm{d}) + \mathrm{Li}(3\mathrm{d}) \rightarrow \mathrm{Li}_2^+ + \mathrm{e}(\varepsilon_v) \quad \text{(AI)}$$

where ε_V is the kinetic energy of the free electrons emitted when Li_2^+ ion formed in the mean relative kinetic energy of the colliding atoms in the beam. Generally, the linear shape of Li_2^+ and the linear and quadratic term exchange show that the only possible mechanism for producing the molecular ion is (AI) at a certain density of Li atomic vapor.

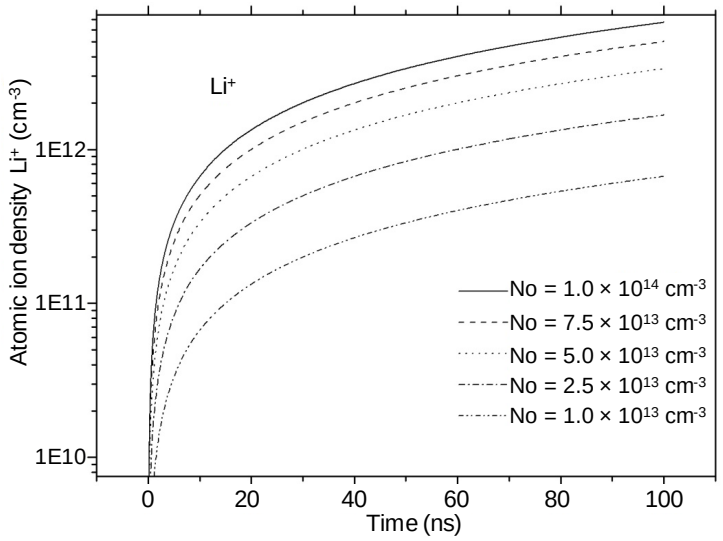

Figure 5. Time evolution of Atomic ion Li^+ at different lithium vapor densities and laser power 1×10^5 W·cm^{-2}.

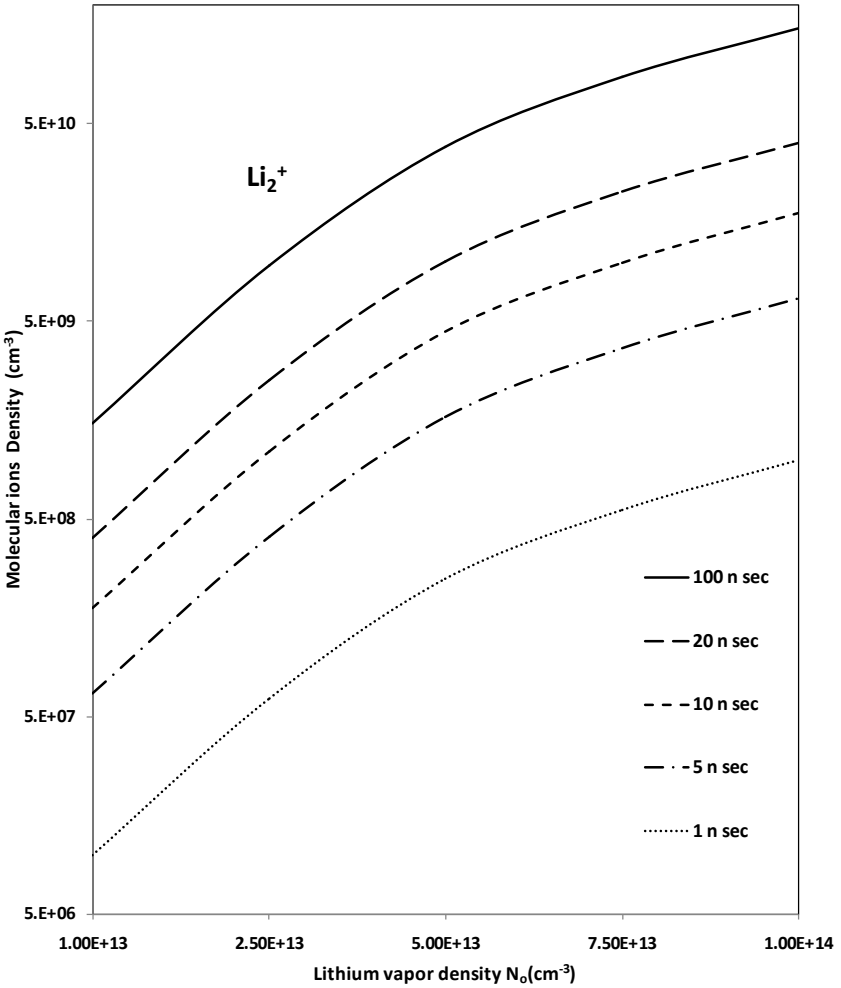

Figure 6. Variation of molecular ion density Li_2^+ with Lithium vapor density N_o at different time intervals and laser power 1×10^5 W·cm^{-2}.

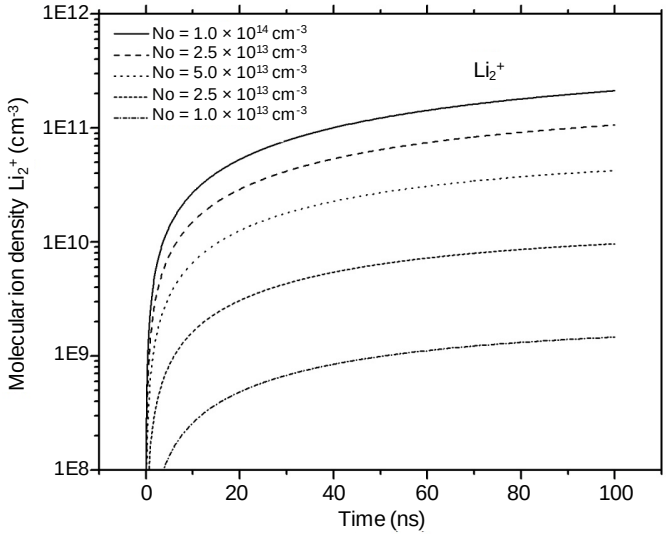

Figure 7. Time evolution of Molecular ion Li_2^+ at different lithium vapor densities and laser power 1×10^5 W·cm^{-2}.

3.6. The Dependence of the Electron Density (N_e) on the Atomic Lithium Vapor and Laser Power

Variation of electrons density with lithium vapor density is shown in **Figure 8**, the curves show that N_e is directly proportional to the lithium vapor at laser power 1×10^5 W·cm^{-2}. Also **Figure 9** shows the dependence of the electron density of the laser power at constant lithium vapor density. From this figure, we note that as the laser increases the density of the electron N_e increases and the curves show the same behavior with descending values of the laser power for the different periods of irradiation time. Moreover, at high laser power greater than 10^5 W·cm^{-2} we note a very fast increase in the electron density. The explanation of this behavior is attributed to the main physical processes which produce the N_e are the photoionization and collisional ionization processes. On the other hand under the resonant radiation the ionization goes from Li(3p), Li(3d) and also from the higher lying states, the photoionization flux from the k_{th} level $\Phi_{ph} = \sigma_{ph}^k n_k F$ is proportional to the ionization cross section σ_{ph}^k, to the level population n_k and to the photon flux density $F = \int I(\upsilon)\,d\upsilon / (h\upsilon)$, where I (W·cm^{-2}) is the incident radiation density. For the conditions under consideration one can expect the maximal population for the states situated near resonant excited Li(3d) level, which is why the total ionization rate is determined by the ionization from Li(3p) and Li(3d) states. The energy gap between these two levels is 0.045 eV.

3.7. The Time Evolution of the Electron Density N_e

The growth rate of electrons N_e as a function of time is indicted in **Figure 10** for different values of lithium vapor density. From this figure, we can see that, the electron density increase up to 20 ns. Immediately after this time the electron density shows a slow increase during the late stages of the interaction. The explanation of the linear growth can be described as follows, after the absorption of two-photon resonance,

$$Li(2s) + 2h\nu_{639.1nm} \rightarrow Li(3d)$$

ions can be created by following paths.

The first is a photoionization of the 3d level:

$$Li(3d) + h\nu_{639.1nm} \rightarrow Li^+ + e$$

The second path is reverse energy pooling or spontaneous decay of Li(3d) to form Li(2p) followed by energy pooling of Li(2p) atoms to form higher excited states like (3d, 3p, …) level followed by photoionization:

$$Li(3d) + Li(2s) \rightarrow Li(2p) + Li(2p)$$

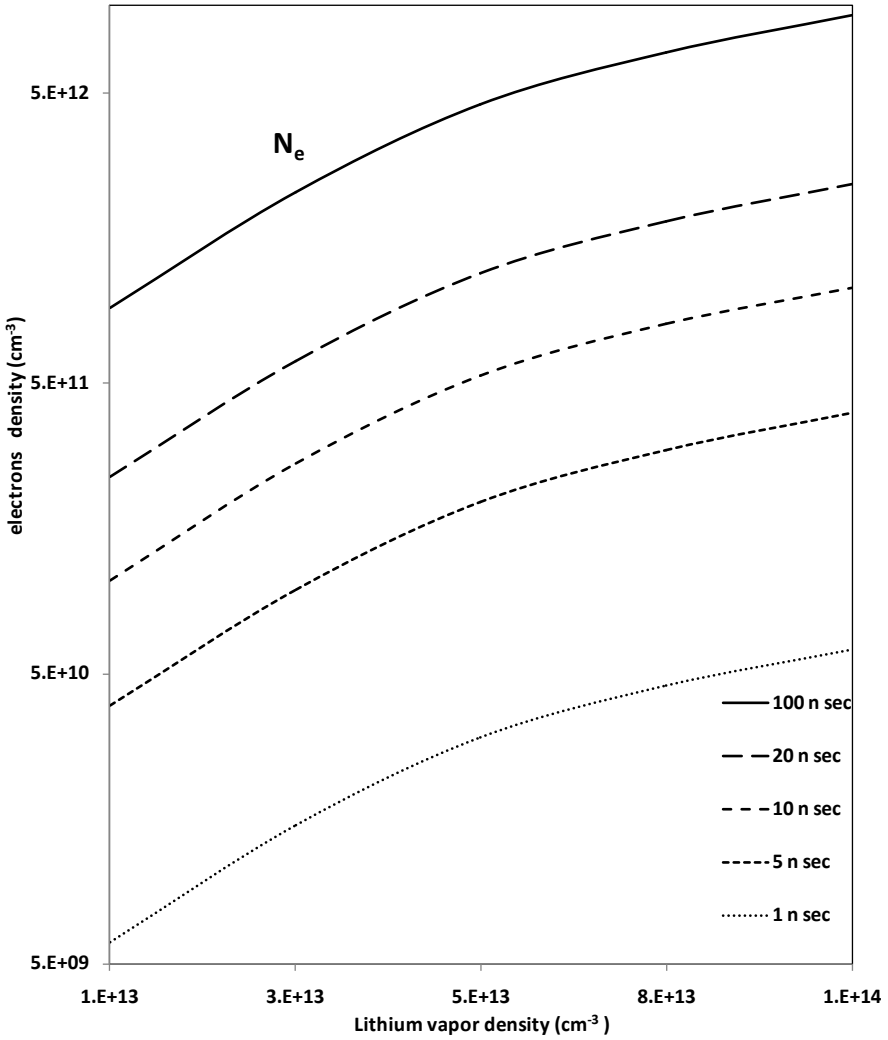

Figure 8. Variation of electrons density N_e with Lithium vapor density N_o at different time intervals and laser power 1×10^5 W·cm^{-2}.

$$\mathrm{Li}(3\mathrm{d}) \rightarrow \mathrm{Li}(2\mathrm{p}) + \mathrm{h}\nu_{610.4\mathrm{nm}}$$

$$\mathrm{Li}(2\mathrm{p}) + \mathrm{Li}(2\mathrm{p}) \rightarrow \mathrm{Li}(3\mathrm{d},3\mathrm{p}) + \mathrm{Li}(2\mathrm{s})$$

$$\mathrm{Li}(3\mathrm{d},3\mathrm{p}) + \mathrm{h}\nu_{670.8} \rightarrow \mathrm{Li}^+ + \mathrm{e}$$

The third one is Penning ionization: $\mathrm{Li}(3\mathrm{d}) + \mathrm{Li}(3\mathrm{d}) + \mathrm{h}\nu_{639.1} \rightarrow \mathrm{Li}(2\mathrm{s}) + \mathrm{Li}^+ + \mathrm{e}$

In general, during the early stages electrons are created at a high rate through photoionization and collisional ionization processes. Beyond this time, the growth rate of the atomic ion becomes slower due to the competition between the generation of the electrons through Penning ionization or photoionization, as well collisional of the ground and excited losses of the ions by radiative recombination and three body recombination [20] [21]. In contrast, photoionization can play a remarkable role at a low ionization degree of the medium, when the basic mechanism of the Li(3p,3d) population are energy pooling collisions: $\mathrm{Li}(2\mathrm{p}) + \mathrm{Li}(2\mathrm{p}) \rightarrow \mathrm{Li}(2\mathrm{s}) + \mathrm{Li}(3\mathrm{p},3\mathrm{d})$ [39]. Through this process electron excitation prevails when $k_{EP}N(2p) > k_{2p\text{-}(3p,3d)}\, n_e$ where k_{EP} is the energy pooling rate coefficient. As far as we know, there is no definite value for this constant for lithium. The considered reaction is an endothermic one. For the pooling reaction with resonant Cs atoms a similar energy gap (ΔE_p ~0.18 eV) the reaction constants are of an order k_{EP} ~(10^{-11} - 10^{-12}) cm^3·s^{-1} [40]. When we employ this value to

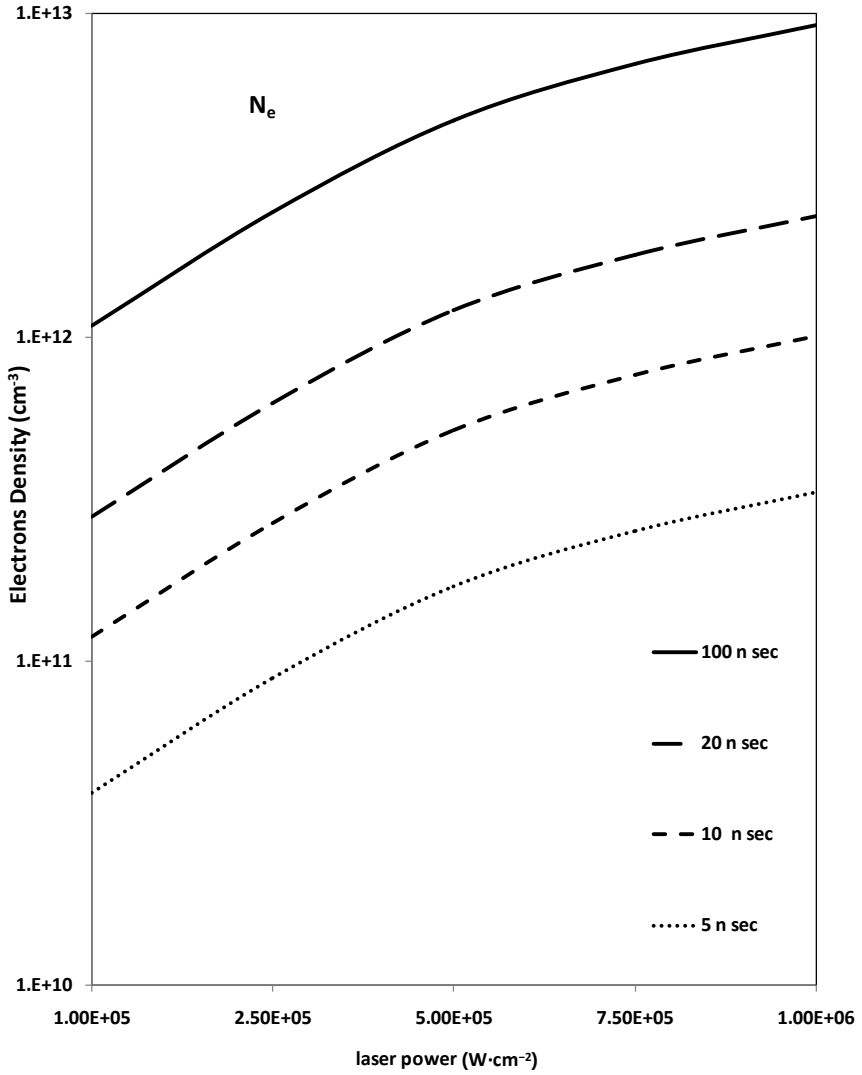

Figure 9. Variation of electrons density N_e with laser power at different time intervals and lithium vapor density 3×10^{13} cm^{-3}.

make estimations for the reaction with lithium we find that under optical saturation potoionization processes can be the dominant processes in ionization processes.

Similarly, energy pooling collisions play a dual role as they deplete the lower states and simultaneously populate the upper states of interest, thus doubling the effect. In fact the two process, (superelastic transfer to the free electrons and energy pooling collisions) work in tandem to create qusicontinuous population inversions.

To give a deeper understanding of the role played by the physical processes in the electron growth rate and to confirm these results we compared our relation with that which obtained by McGeoch [24]. He applied his simple kinetic model of optically pumped lithium plasma to calculate the time evolution of the electron density which created during the interaction of lithium vapor with laser radiation. From **Figure 11** it is seen that our results showed the same trend as those calculated by McGeoch [24], where their values display reasonable consistency over the whole range time. This in turn verified the validity of the model to investigate the Electron energy distribution function (EEDF) in lithium vapor excitation at 2s→3d two-photon resonance.

4. Conclusion

We have carried out a computational study of the influence of collisional ionization and collisional excitation processes which occur in lithium vapour under two-photon excitation of the Li(3d) state at 639.1 nm. We have

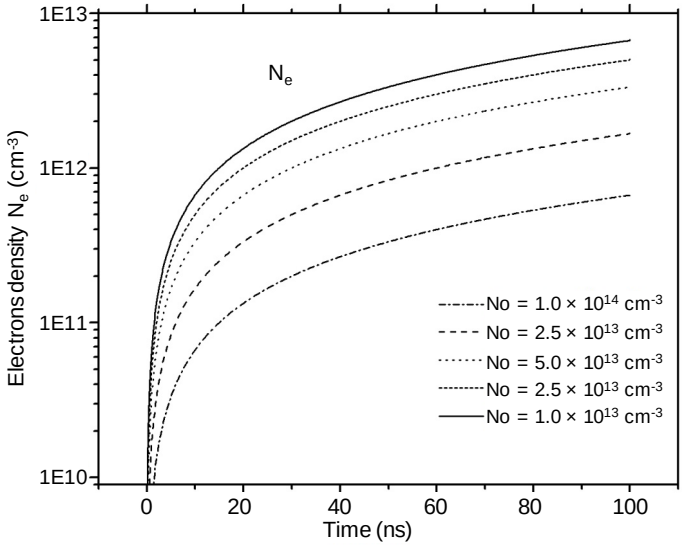

Figure 10. Time evolution of electrons density N_e at different lithium vapor densities and laser power 1×10^5 W·cm^{-2}.

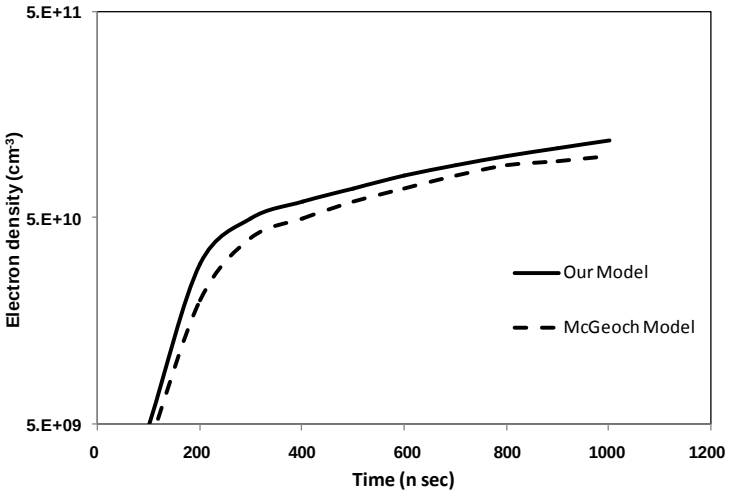

Figure 11. Comparison between the calculated Electron density of our model and that obtained by McGeoch [24] model at Laser pulse = 20 ns and lithium vapor density Li = 1×10^{13} cm^{-3}.

calculated the electron energy distribution function as well as the molecular ions and atomic ions for lithium atom densities in the range (10^{13} - 10^{14} cm^{-3}) and laser powers (10^5 - 10^6 W·cm^{-2}). The results confirm a satisfactory description of the experimentally observed behavior. At atomic density of 10^{14} cm^{-3} radiation population of the Li(2p) state dominates over the collisional energy transfer (REP). The reverse energy pooling as a source for large pool of Li(2p) atoms could be important at large atom densities. The nonlinear dependence of the electron energy distribution function on the lithium vapor density indicates that collisional processes, such as laser induced Penning ionization, associative ionization, Photoionization, as well as energy pooling collisions (which play role in populating the 3p and 3d states) form the plasma. The high energy of the EEDF had a non-equilibrium shape. This was caused by relaxation of fast electrons produced by super-elastic collisions with residual excited atoms. The model may be useful in a laser induced plasma or discharge experiments.

References

[1] Gorbunov, N.A., Grochola, A., Kruk, P., Pietruczuk, A. and Stacewicz, T. (2002) Studies of Electron Energy Distribu-

tion in Plasma Produced by a Resonant Laser Pulse. *Plasma Sources Science and Technology*, **11**, 492-497. http://dx.doi.org/10.1088/0963-0252/11/4/316

[2] Hassanien, A., Sizyuk, V. and Sizuk, T. (2011) The Effect of Critical Plasma Densities of Laser-Produced Plasma on Production of Extreme Ultraviolet Radiation. *IEEE Transations on Plasma Science*, **39**, 2810-2811.

[3] Bartirmoro, R., Bombarada, F. and Giannella, R. (1985) Spectroscopic Study of Nonthermal Plasmas. *Spectroscopic Study of Nonthermal Plasmas*, **32**, 531-537. http://dx.doi.org/10.1103/PhysRevA.32.531

[4] Liu, J.M., De Groot, J.S., Matte, J.P., Johnston, T.W., and Drake, R.P. (1994) Electron Heat Transport with Non-Maxwellian Distributions. *Physics of Plasmas*, **1**, 3570-3576. http://dx.doi.org/10.1063/1.870892

[5] Zhidkov, A.G., Sasaki, A., Tajima, T., Auguste, T., D'Olivera, P., Hulin, S., Monot, P., Faenov, A.Y., Pikuz, T.A. and Skoobelev, I.Y. (1999) Direct Spectroscopic Observation of Multiple-Charged-Ion Acceleration by an Intense Femto-second-Pulse Laser, *Physical Review E*, **60**,3273-3278. http://dx.doi.org/10.1103/PhysRevE.60.3273

[6] Zhidkov, A.G., Sasaki, A., Fukumoto, I., Tajima, T., Auguste, T., D'Olivera, P., Hulin, S., Monot, P., Faenov, A.Y., Pikuz, T.A. and Skobelev, I.Y. (2001) Pulse Duration Effect on the Distribution of Energetic Particles Produced by Intense Femtosecond Laser Pulses Irradiating Solids. *Physics of Plasmas*, **8**, 3718-3723.

[7] Whitney, K.G. and Pulsifier, P.E. (1993) Plasma Conditions for Non-Maxwellian Electron Distributions in High Current Discharges and Laser-Produced Plasmas. *Physical Review E*, **47**, 1968-1976. http://dx.doi.org/10.1103/PhysRevE.47.1968

[8] Choi, P., Deeney, C, and Wong, C.S. (1988) Absolute Timing of a Relativistic Electron Beam in a Plasma Focus. *Physics Letters A*, **128**, 80-83. http://dx.doi.org/10.1016/0375-9601(88)91048-1

[9] Kantsyrev, V.L., Fedin, D.A., Shlyaptseva, A.S., Hansen, S., Chamberlain, D. and Ouart, N. (2003) Energetic Electron Beam Generation and Anisotropy of Spectra and Spatial Distribution of Hard X-Ray Emission from 0.9 - 1.0 MA High-Z X-Pinches. *Physics of Plasmas*, **10**, 2519-2526. http://dx.doi.org/10.1063/1.1572489

[10] Pereira, N.R. and Whitney, K.G. (1988) Non-Maxwellian Electron-Energy Distribution Due to Inelastic Collisions in a Z-Pinch Plasma. *Physical Review A*, **38**, 319-327. http://dx.doi.org/10.1103/PhysRevA.38.319

[11] McTienan, J.M. and Petrosian, V. (1990) The Behavior of Beams of Relativistic Nonthermal Electrons under the Influence of Collisions and Synchrotron Losses. *Astrophysical Journal*, **359**, 541-546.

[12] Kato, T., Fujiwara, T. and Hanaoka, Y. (1998) X-Ray Spectral Analysis of *Yohkoh* Bragg Crystal Spectrograph Data on a 1992 September 6 Flare: The Blueshift Component and Ion Abundances. *Astrophysical Journal*, **492**, 822-832. http://dx.doi.org/10.1086/305047

[13] Baring, M.G. (1991) The Collisional Acceleration of Relativistic Electrons in the Central Regions of Active Galactic Nuclei. *Monthly Notices of the Royal Astronomical Society*, **253**, 388-400. http://dx.doi.org/10.1093/mnras/253.3.388

[14] Gorbunov, A.N. and Stacewicz, T. (2000) Photo EMF Observed upon the Laser Resonance Excitation of Sodium Vapors. *Technical Physics Letters*, **26**, 654-655. http://dx.doi.org/10.1134/1.1307803

[15] Gorbunov, A.N. and Stacewicz, T. (2001) Observation of an Electromotive Force in a Decaying Photoresonance Plasma of Sodium Vapors. *High Temperature*, **39**, 623-625. http://dx.doi.org/10.1023/A:1017956827981

[16] Gorbunov, A.N., Melnikov, S., Smurov, I. and Bray, I. (2001) Ionization Kinetics of Optically Excited Lithium Vapor under Conditions of Negative Electron Mobility. *Journal of Physics D*: *Applied Physics*, **34**, 1379-1388. http://dx.doi.org/10.1088/0022-3727/34/9/315

[17] Stwalley, W.C. and Bahns, J.T. (1993) Atomic, Molecular, and Photonic Processes in Laser-Induced Plasmas in Alkali Metal Vapors. *Laser and Particle Beams*, **11**, 185-204.

[18] Veza, D. and Sansonetti, C.J. (1992) Ionization of Lithium Vapor by CW Quasiresonant Laser Light. *Zeitschrift für Physik D Atoms, Molecules and Clusters*, **22**, 463-470. http://dx.doi.org/10.1007/BF01426088

[19] Koch, M.E. and Collins, C.B. (1979) Space-Charge Ion Detection of Multiphoton Absorption Phenomena in Lithium Vapor. *Physical Review A*, **19**, 1098-1105. http://dx.doi.org/10.1103/PhysRevA.19.1098

[20] Skenderovic, H., Labazan, I., Milosevic, S. and Pichler, G. (2000) Laser-Ignited Glow Discharge in Lithium Vapor. *Physical Review A*, **62**, 0527071-7.

[21] Labazan, I. and Milosevic, S. (2000) Lithium Vapour Excitation at 2S→3D Two-Photon Resonance. *European Physical Journal D*, **8**, 41-47.

[22] Measures, R.M. and Cardinal, P.G. (1981) Laser Ionization Based on Resonance Saturation. A Simple Model Description. *Physical Review A*, **23**, 804-815. http://dx.doi.org/10.1103/PhysRevA.23.804

[23] Stacewicz, T. and Topulos, G. (1988) Ionization of Sodium Vapour by Nanosecond Resonant Laser Pulses. *Physica Scripta*, **38**, 560-563. http://dx.doi.org/10.1088/0031-8949/38/4/010

[24] McGeoch, M.W. (1989) Processes in a Lithium Negative Ion Source. *SPIE Symposium on Innovative Science and*

Technology, Los Angeles, January 1989, 1-26.

[25] Mahmoud, M.A. (2008) Kinetics of Rb^+_2 and Rb^+ Formation in Laser-Excited Rubidium Vapor. *Central European Journal of Physics*, **6**, 530-538. http://dx.doi.org/10.2478/s11534-008-0074-5

[26] Mahmoud, M.A., El Tabal, A. and Nady, M. (2012) Collisional Ionization in Lithium Vapor Excited by Nanosecond Laser Pulses. *Acta Physica Polinica A*, **122**, 71-77.

[27] Bezuglov, N.N., Klyucharev, A.N. and Sheverev, V.A. (1987) Associative Ionization Rate Constants Measured in Cell and Beam Experiments. *Journal of Physics B*: *Atomic and Molecular Physics*, **20**, 2497-2513. http://dx.doi.org/10.1088/0022-3700/20/11/018

[28] Mahmoud, M.A. (2005) Electron Energy Distribution Function in Laser-Excited Rubidium Atoms. *Journal of Physics B*: *Atomic, Molecular and Optical Physics*, **38**, 1545-1556. http://dx.doi.org/10.1088/0953-4075/38/10/012

[29] Oxenius, J. (1986) Kinetic Theory of Particles and Photons. Springer, Berlin. http://dx.doi.org/10.1007/978-3-642-70728-5

[30] Vriens, L. and Smeets, A.H.M. (1980) Cross-Section and Rate Formulas for Electron-Impact Ionization, Excitation, Deexcitation, and Total Depopulation of Excited Atoms. *Physical Review A*, **22**, 940-951. http://dx.doi.org/10.1103/PhysRevA.22.940

[31] Drawin, W.H. (1967) Collision and Transport Cross—Sections. Association Euratom CEA, 92 Fontenay-aux Roses, France, 496-506.

[32] Tisone, G.C. and Hargis Jr., P.J. (1987) Laser Absorption and Fluorescence Studies of the Lithium 2S - 3D Transition. *AIP Conference Proceedings*, Vol. 160, AIP Press, New York, 404-417.

[33] Wiese, W.L., Smith, M.W. and Glennon, B.M. (1966) Atomic Transition Probabilities. Vol. I, National Bureau of Standards, Washington, DC, 17.

[34] Wiese, W.L. and Fuhr, J.R. (2009) Accurate Atomic Transition Probabilities for Hydrogen, Helium, and Lithium. *Journal of Physical and Chemical Reference Data*, **38**, 565. http://dx.doi.org/10.1063/1.3077727

[35] McGeoch, M.W., Schiler, R.E. and Chawla, G.K. (1988) Associative Ionization with Cold Rydberg Lithium Atoms. *Physical Review Letters*, **61**, 2088-2091. http://dx.doi.org/10.1103/PhysRevLett.61.2088

[36] Jabbour, Z.J., Namiotka, R.K., Huennekens, J., Allegrini, M., Milosevic, S. and De Tomasi, F. (1996) Energy Pooling Collisions in Cesium: $6P_J$+ 6PJ→6S+ (nl= 7P, 6D, 8S, 4F). *Physical Review A*, **54**, 1372-1384.

[37] De Filippo, G., Guldberg-Kjaer, S., Milosevic, S., Pedersen, J.O.P. and Allegrini, M. (1998) Reverse Energy-Pooling in K-Na Mixture. *Physical Review A*, **57**, 255-266.

[38] Aymar, M., Luc-Koenig, E. and Combet Farnoux, F. (1976) Theoretical Investigation on Photoionization from Rydberg States of Lithium, Sodium and Potassium. *Journal of Physics B*: *Atomic and Molecular Physics*, **9**, 1279-1291. http://dx.doi.org/10.1088/0022-3700/9/8/013

[39] He, C. and Bernheim, R.A. (1992) Energy Transfer and Energy Pooling from 2 ^{2}P 3/2,1/2 Excited Li Atoms in Li Vapor. *Chemical Physics Letters*, **190**, 494-506.

[40] Klucharev, A.N. and Vujnovic, A. (1990) Chemi-Ionization in Thermal-Energy Binary Collisions of Optically Excited Atoms. *Physics Reports*, **185**, 57-81. http://dx.doi.org/10.1016/0370-1573(90)90112-F

Scientific Research Publishing (SCIRP) is one of the largest Open Access journal publishers. It is currently publishing more than 200 open access, online, peer-reviewed journals covering a wide range of academic disciplines. SCIRP serves the worldwide academic communities and contributes to the progress and application of science with its publication.

Other selected journals from SCIRP are listed as below. Submit your manuscript to us via either submit@scirp.org or Online Submission Portal.